

ORIGINAL ARTICLE

Dual inhibition of SRC and Aurora kinases induces postmitotic attachment defects and cell death

V Ratushny^{1,2}, HB Pathak^{1,4}, N Beeharry¹, N Tikhmyanova¹, F Xiao¹, T Li¹, S Litwin¹, DC Connolly¹, TJ Yen¹, LM Weiner³, AK Godwin^{1,4} and EA Golemis¹

¹Fox Chase Cancer Center, Philadelphia, PA, USA; ²Program in Molecular and Cell Biology and Genetics, Drexel University College of Medicine, Philadelphia, PA, USA and ³Lombardi Comprehensive Cancer Center, Georgetown University Medical Center, Washington, DC, USA

Increased activity of SRC family kinases promotes tumor invasion and metastasis, and overexpression of the mitotic regulator Aurora kinase A (AURKA) drives tumor aneuploidy and chromosomal instability. These functions nominate SRC and AURKA as valuable therapeutic targets for cancer, and inhibitors for SRC and Aurora kinases are now being used in the clinic. In this study, we demonstrate potent synergy between multiple inhibitors of Aurora and SRC kinases in ovarian and colorectal cancer cell lines, but not in normal ovarian epithelial cell lines. Combination of Aurora and SRC inhibitors selectively killed cells that have undergone a preceding aberrant mitosis, and was associated with a postmitotic reattachment defect, and selective removal of aneuploid cell populations. Combined inhibition of Aurora kinase and SRC potentiated dasatinib-dependent loss of activated (Y⁴¹⁶-phosphorylated) SRC. SRC and AURKA share a common interaction partner, NEDD9, which serves as a scaffolding protein with activities in cell attachment and mitotic control, suggesting SRC and AURKA might interact directly. *In vitro*, we observed physical interaction and mutual cross-phosphorylation between SRC and AURKA that enhanced SRC kinase activity. Together, these findings suggest that combination of SRC and Aurora-targeting inhibitors in the clinic may be a productive strategy.

Oncogene (2012) 31, 1217–1227; doi:10.1038/onc.2011.314; published online 25 July 2011

Keywords: SRC; NEDD9; Aurora; drug; mitosis; attachment

Introduction

Substantial effort has been devoted to the creation of protein-targeted biological therapeutics intended

to prevent the growth and metastasis of tumor cells (Cao and Liu, 2007; Pfeiffer *et al.*, 2007). However, pre-clinical testing and early phase trials have generally indicated that few of these agents used as monotherapies have produced strong gains in blocking tumor growth (Brandsma and van den Bent, 2007; Wong and Goodin, 2009). An emerging strategy in overcoming resistance is the identification of novel combination therapies involving targeted agents, as these often have enhanced clinical efficacy (Bagnyukova *et al.*, 2010). We now describe a novel strategy involving the combination of inhibitors of SRC and Aurora kinases.

The tyrosine kinase SRC regulates cell proliferation, survival, cytoskeleton, cell–cell contacts and cell-matrix attachments at focal adhesions (Yeatman, 2004; Guarino, 2010). At focal adhesions, SRC forms an activated complex with focal adhesion kinase and scaffolding proteins such as NEDD9 (Yeatman, 2004) to regulate focal adhesion turnover, stimulating downstream effector pathways that reorganize the cytoskeleton during migration. SRC also becomes hyperactive at the G2/M transition, and phosphorylates substrates that promote focal adhesion disassembly and facilitate the cell rounding phenotype characteristic of mitosis (Mustelin and Hunter, 2002). SRC is overexpressed in a large percentage of human tumors including colorectal, breast, ovarian, prostate, pancreas, lung carcinoma, glioma, melanoma, head and neck, and different types of sarcoma (Shor *et al.*, 2007; Guarino, 2010). Interestingly, SRC is only rarely mutated in tumors, suggesting aberrant interactions with partner proteins may contribute to its increased activity. Activated SRC supports tumor growth, invasion and metastasis (Yeatman, 2004).

Aurora serine/threonine kinases (Aurora-A/AURKA, Aurora-B/AURKB, and Aurora-C/AURKC) are best known for roles in M-phase (Keen and Taylor, 2004; Gautschi *et al.*, 2008), although recent publications have begun to identify roles for AURKA in interphase cells (Pugacheva *et al.*, 2007; Plotnikova *et al.*, 2010; Plotnikova and Golemis, 2011). AURKA is best known for regulating mitotic entry and progression, influencing centrosome maturation and separation, bipolar-spindle assembly, chromosomal alignment on the metaphase plate and cytokinesis (Glover *et al.*, 1995; Dutertre *et al.*, 2002). As with SRC, AURKA protein overexpression often occurs in ovarian, colorectal, pancreatic, liver,

Correspondence: Dr EA Golemis, Developmental Therapeutics, Fox Chase Cancer Center, 333 Cottman Ave, W406, Philadelphia, PA 19111, USA.

E-mail: EA_Golemis@fccc.edu

⁴Current address: University of Kansas Medical Center, Kansas City, KS 66106, USA.

Received 1 February 2011; revised 2 June 2011; accepted 18 June 2011; published online 25 July 2011

bladder and gastric cancers, and is generally associated with genomic instability and aneuploidy, a higher tumor grade and a poor prognosis (Bischoff *et al.*, 1998; Giet *et al.*, 2005). Exogenous overexpression of AURKA either *in vitro* or *in vivo* transforms rodent fibroblast cells and induces tetraploidization, failed cytokinesis and genomic instability. Overexpressed AURKA also affects the DNA damage-induced G2 checkpoint, and the mitotic spindle checkpoint (Anand *et al.*, 2003). AURKB is rarely overexpressed in tumors, but has important roles in regulating kinetochore and chromosome segregation in mitosis (Ditchfield *et al.*, 2003). In contrast, AURKC has limited expression, and has primarily been studied in the context of meiotic cell division and early development (Fernandez-Miranda *et al.*, 2011).

Several lines of evidence suggested the possibility of functional or direct physical interactions for SRC and AURKA. Both proteins interact with a common partner, NEDD9, with these interactions contributing to activation of each kinase (Minegishi *et al.*, 1996; Pugacheva and Golemis, 2005; Pugacheva *et al.*, 2007). Besides its role in mitosis, AURKA activity has recently been identified as regulating cell migration, similar to NEDD9 and SRC (Guan *et al.*, 2007). An emerging paradigm for the design of combinatorial therapies takes as its model synthetic lethal analyses from lower organisms. These studies have established that dual inhibition of proteins operating together or in parallel pathways is often particularly effective in reducing signaling function, to potential therapeutic gain (Friedman and Perrimon, 2007). With this goal, we have here assessed the consequences of dual inhibition of Aurora kinases and SRC. We here report that multiple SRC and Aurora inhibitors synergize strongly to promote cell killing in cancer cell lines. This cell killing is associated with a postmitotic attachment defect, clearance of aneuploid cell populations and hypoactive SRC. We also establish that SRC and AURKA directly associate and phosphorylate each other *in vitro*, supporting the idea of direct interaction. These and other findings provide an initial justification for combining SRC and Aurora inhibitors in the clinic.

Results

Consistent synergy between inhibitors of SRC and Aurora kinases in transformed but not normal cell lines

Dasatinib is selective for SRC family kinases (SRC, YES and LCK) and BCR-ABL, with activity at higher concentrations as an inhibitor of PDGFR β , c-KIT and p38 (Lombardo *et al.*, 2004). We initially assessed the combination of dasatinib, and the Aurora kinase inhibitor PHA-680632 (Soncini *et al.*, 2006) in limiting cell growth of a panel of human epithelial ovarian cancer cell lines (Figure 1a, Supplementary Table 1), and normal primary human ovarian surface epithelial (HOSE) cells (Figure 1b). Chou-Talalay analysis of results indicated that at multiple different drug-combination ratios, dasatinib and PHA-680632 synergized

to restrict the growth of 8/8 epithelial ovarian cancer cell lines, but 0/3 HOSE cell lines. Similar synergy was obtained using either of two alternative small molecule inhibitors of Aurora kinases (MLN8237 or C1368, both preferentially inhibiting AURKA) in combination with dasatinib, or an alternative small molecule inhibitor of SRC kinases (PP2) in combination with PHA-680632 (Figure 1c). Potent synergy was also observed in 3/3 colorectal cancer cell lines, including the RAS-mutated DLD1 cell line and its RAS wild-type isogenic counterpart, DKS8 (Figure 1c).

As separate measures of efficacy of the dasatinib-PHA630632 combination, we performed clonogenic assays (Figures 2a and b) and assessed colony formation on matrigel (Figures 2c and d). By both measures, treatment of cells with the combination resulted in significantly reduced colony size and total number of colonies versus treatment with either single agent at the same dose. Further, cells within matrigel colonies treated with the drug combination were much more positive for cleaved caspase-3 (Figure 2e), indicating the occurrence of apoptotic cell death, rather than solely cytostasis.

Dual inhibition of Aurora and SRC kinases selectively reduces accumulation of aneuploid cells associated with Aurora inhibition

To begin to explore the molecular basis for the strong synergy in growth inhibition, we investigated the consequences of combining dasatinib and PHA-680632 on cell-cycle progression (Figure 3a). Treatment of thymidine-synchronized OVCAR10 cells with dasatinib caused G1 accumulation ($57 \pm 11\%$ of total cells versus $45 \pm 3\%$ for vehicle treated cells) within 24 h. Treatment with PHA-680632 caused accumulation of cells in the 4N (G2/M) compartment ($38 \pm 6\%$ of total cells versus $32 \pm 2\%$ for vehicle-treated cells), and also led to the appearance of a significant $>4N$ cell population ($30 \pm 4\%$ of total cells versus $5 \pm 2\%$ for vehicle-treated cells). Treatment with the dasatinib/PHA-680632 combination resembled treatment with PHA-680632, but further increased the proportion of 4N cells (to $46 \pm 8\%$) versus PHA-680632 alone. Intriguingly, the combination significantly and selectively reduced the hyperploid $>4N$ population at 19 and 24 h relative to PHA-680632 treatment alone (to 7 ± 2 and $11 \pm 2\%$, respectively, versus 18 ± 2 and $30 \pm 4\%$; $P=0.0048$ and 0.0015). Similar results were obtained in a second cell line, PEO-1 (Supplementary Figure S1), but were not observed in HOSE cells treated with the same concentrations of drugs (Figure 3b). Further, although a $>4N$ hyperploid population was induced by treatment of cells with inhibitors selective for AURKA (MLN8257) or AURKB (AZD1152), only the combination of dasatinib with MLN8257 selectively reduced this population of cells (Figure 3c), suggesting a specific interaction between dasatinib targets and AURKA.

The fluorescence-activated cell sorting results suggested that the drug combination-induced lethality specifically involves mitotic progression. To better address mitotic progression after drug treatment, live

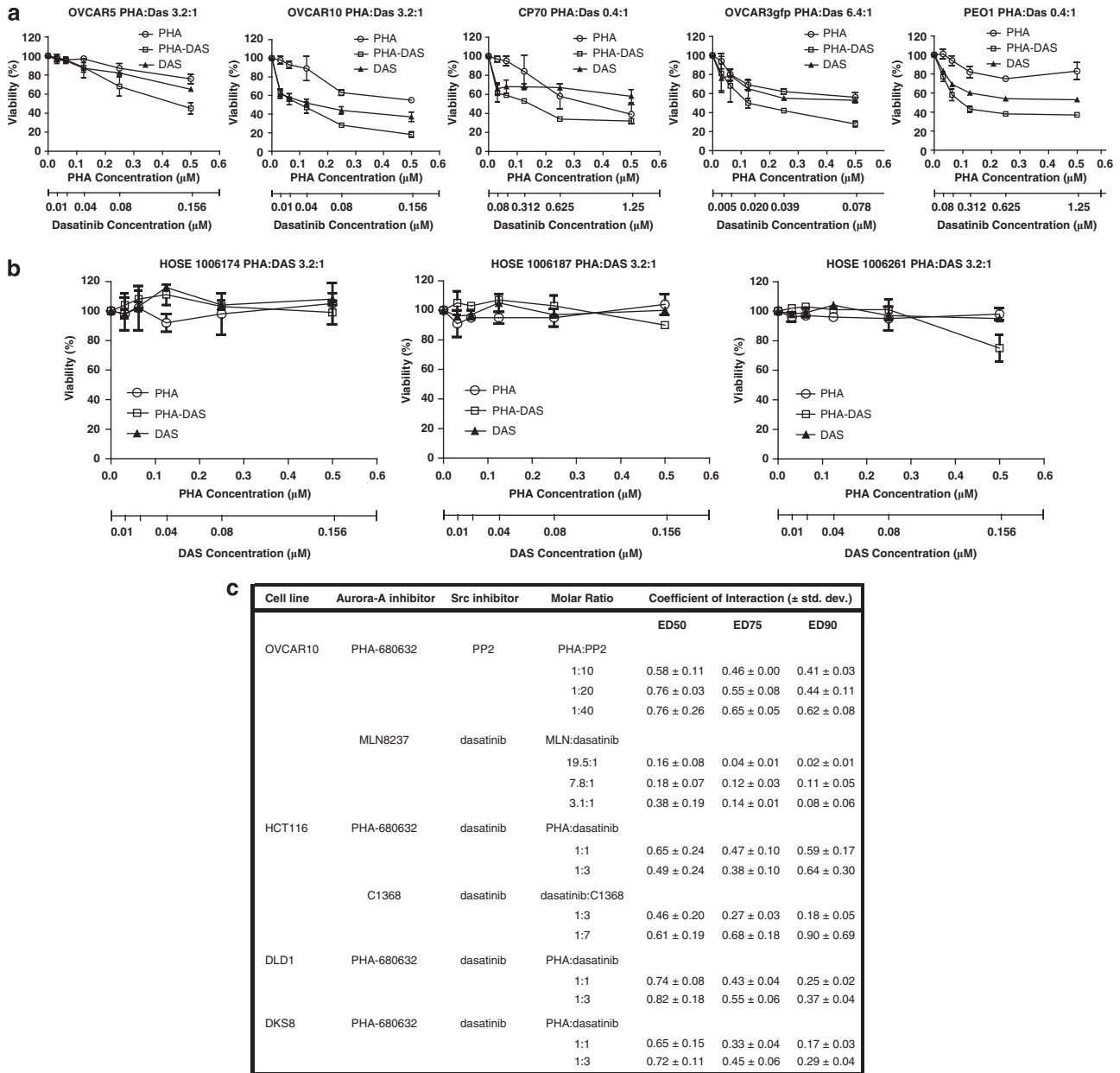


Figure 1 Consistent and strong synergy between inhibitors of SRC and Aurora kinases in transformed but not normal cell lines. (a) Synergy between PHA-680632 (PHA) and dasatinib (DAS) was tested by CellTiter Blue assay in 8 ovarian cancer cell lines and viability curves for five representative cell lines were displayed (refer to Supplementary Table 1 for a complete list of cell lines tested). (b) Synergy between PHA-680632 and dasatinib was tested in three normal primary HOSE cell lines, and viability curves for the individual drugs or the drug combination were plotted. (c) A coefficient of interaction (CI) value of > 1 indicates antagonism; CI = 1 indicates additive effects; CI of < 0.9 indicates synergy; and CI of < 0.5 indicates strong synergy. CI values for combinations of Aurora (PHA-680632, MLN8237, C1368) and SRC (dasatinib, PP2) inhibitors in human ovarian (OVCAR10) or human colorectal carcinoma (HCT116, DLD1 (RAS-mutated), DKS8 (RAS wild-type isogenic to DLD1)) cell lines.

cell imaging was used to characterize in detail the progression through mitosis of thymidine-synchronized (S-phase arrested) OVCAR10 cells that stably expressed GFP fused to histone H2B, to allow visualization of nuclei and chromosomes. Drugs were added 3 h after removal of thymidine. The time required for entry to mitosis, measured as chromosomal condensation, was equivalent among the treatment groups (5.28 ± 1.68 h for vehicle, 5.49 ± 1.52 h for PHA-680632, 4.63 ± 2.10 h

for dasatinib, and 5.42 ± 1.67 h for the dasatinib/PHA-680632 combination) (Figure 3d). PHA-680632 treatment slightly decreased the percent of cells entering mitosis, but this effect was eliminated when cells were treated with the drug combination (Figure 3e). Treatment of cells with PHA-680632 increased the overall duration of mitosis (from 93.6 to 139.4 min), which was similar to the delay seen in cells treated with PHA-680632 plus dasatinib (149.2 min) (Figure 3f).

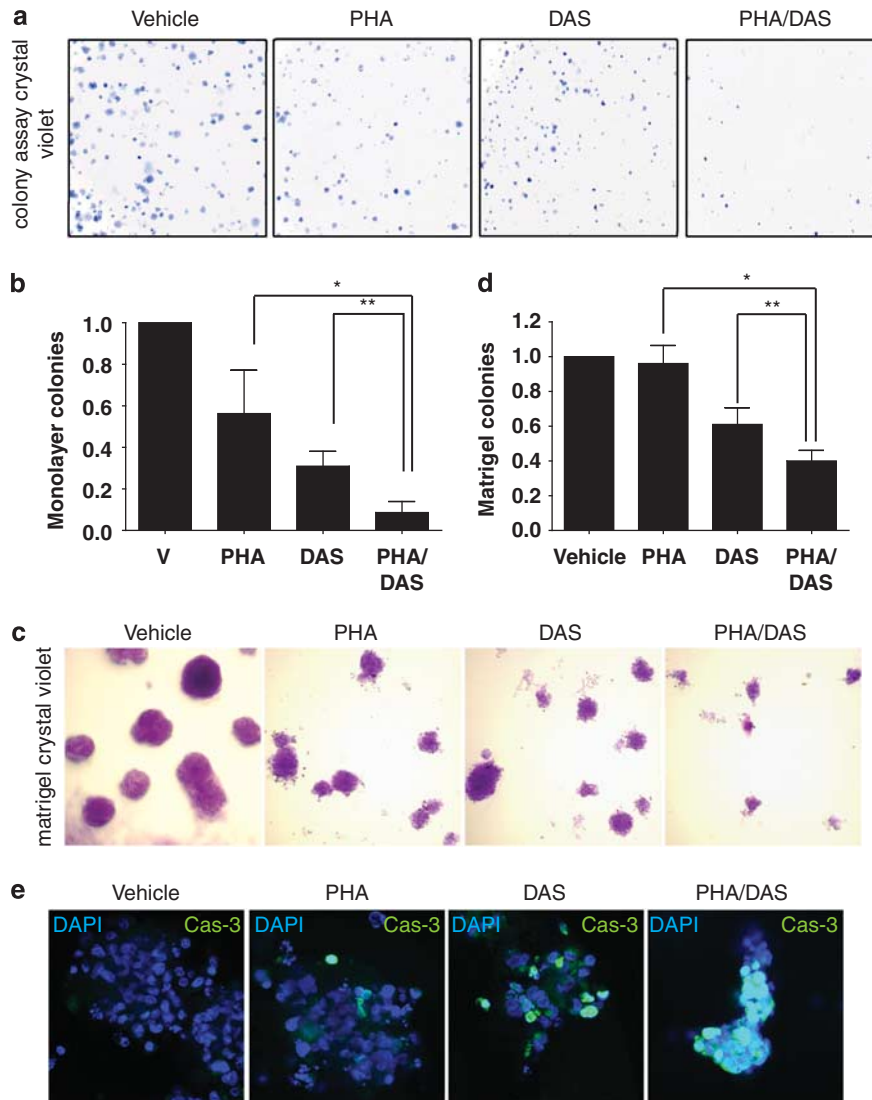


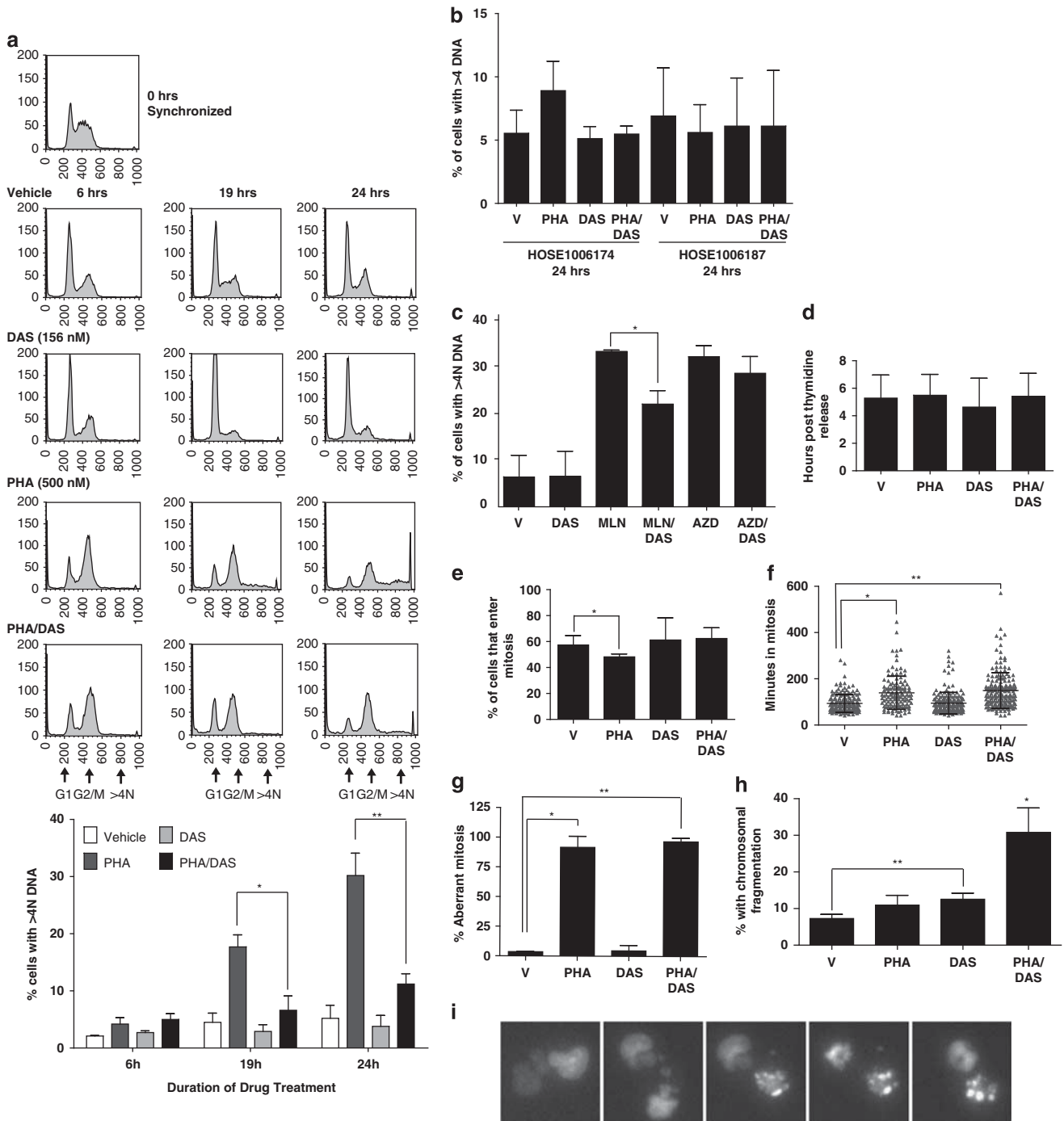
Figure 2 Efficacy of dasatinib-PHA680632 combination in clonogenic and matrigel assays. **(a)** Representative colonies of OVCAR10 at 12 days of growth after treatment with indicated drugs. **(b)** Quantification of monolayer colonies from three independent clonogenic experiments performed as in **a**. Data are represented as percentage clonogenic survival from vehicle-treated control cells ($100\% \pm$ s.d. of mean. $*P=0.0093$; $**P=0.0061$). **(c)** Representative colonies of cells after growth for 8 days with drug treatment in matrigel. **(d)** Quantification of reduction in number of matrigel colonies relative to vehicle-treated cells. $*P=0.00065$; $**P=0.03035$. **(e)** Representative image of caspase-3-stained colonies after growth in matrigel as in **c**.

Figure 3 Dual inhibition of Aurora and SRC kinases specifically eliminates hyperloid cells. **(a)** A representative FACS analysis of synchronized OVCAR10 cells treated with vehicle (V), 500 nM PHA-680632 (PHA), 156 nM dasatinib (DAS), or the drug combination. Cell-cycle profiles were evaluated at times indicated after addition of drug. Graph below represents quantification of cells with $>4N$ DNA from at least two independent repetitions of these $*P=0.0048$, $**P=0.0015$. **(b)** Experiment shown is the same as for graph in **a**, based on 24 h incubation of two independent HOSE cell lines with indicated drugs. **(c)** Experiment shown is same as **a**, **b**, but performed following treatment of OVCAR10 cells with MLN8237 (targeting AURKA) or AZD1152 (targeting AURKB); $*P=0.0164$. **(d)** No significant difference in the time required for cells to enter mitosis between the drug treatment groups. Time recorded in hours post thymidine release of cells. Data represent averages and standard deviations from three time-lapse microscopy experiments. **(e)** PHA-680632 reduces the number of cells that enter mitosis, scored as chromosomal condensation, over 48 h of observation. Data are merged from three independent experiments; $*P=0.039$. **(f)** Treatment with 500 nM PHA-680632 ($*P<0.0001$) and PHA-680632 plus 156 nM dasatinib ($**P<0.0001$) increase duration of mitosis. Triangles represent individual cells counted and the horizontal line with error bars represents means and standard deviations. Y-axis represents the duration of mitosis as measured by minutes from chromatin condensation to chromatin decondensation. Combined data are shown from three time-lapse microscopy experiments. **(g)** Treatment with PHA-680632 ($*P$ versus vehicle <0.0001) or with PHA-680632 plus dasatinib ($**P$ versus vehicle <0.0001) significantly induces aberrant mitosis in OVCAR10 cells. **(h)** Chromosomal fragmentation in OVCAR10 cells within 48 h after treatment with drugs (500 nM PHA-680632 or 156 nM dasatinib) or drug combinations. Combination treatment strongly induced chromosomal fragmentation versus treatment with vehicle alone ($*P<0.0001$), 500 nM PHA-680632 alone ($*P<0.0001$), or 156 nM dasatinib alone ($*P<0.0001$). Dasatinib alone modestly induced chromosomal fragmentation versus vehicle ($**P=0.04026$). **(i)** Representative montage of phenotypic chromosomal fragmentation of OVCAR10 cells in time-lapse microscopy experiments, which were quantitated in **h**.

PHA-680632 treatment induced a high frequency of cells that underwent aberrant mitosis with cleavage furrow regression to produce a binucleate single progeny (Figure 3g, Supplementary Figure S2), but this frequency was not further enhanced by addition of dasatinib. A marked increase in cells undergoing abrupt condensation and fragmentation of chromosomal material, to produce the pyknotic nuclei typically associated with apoptotic cells, was evident in live-cell imaging of combination-treated cells (Figures 3h and i).

Dual inhibition of Aurora and SRC kinases selectively kills cells that have undergone defective mitoses and failed to reattach

The preceding results might indicate the drug combination increased the killing of the postmitotic, hyperplod cells or caused death during mitosis of cells that would otherwise be destined to become hyperplod. To discriminate between these possibilities, we performed a subgroup analysis of cells that underwent cell death, as defined by nuclear fragmentation and cellular



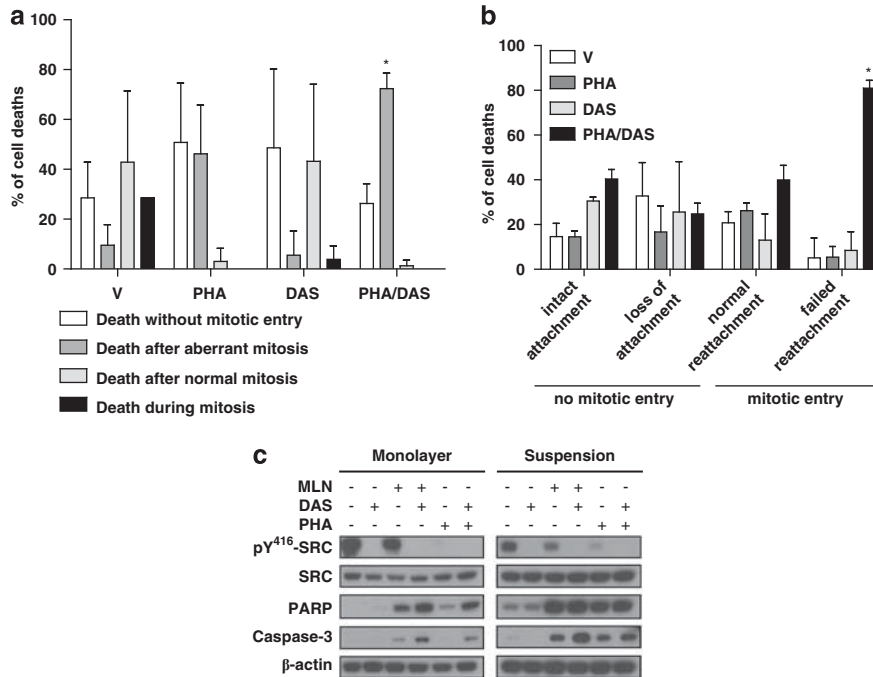


Figure 4 Dual inhibition of Aurora-A and SRC kinases selectively kills cells that have undergone defective mitoses. (a) Treatment with the PHA-680632 plus dasatinib combination caused most cell deaths after an abnormal mitosis ($*P$ versus dasatinib <0.0001 , $*P$ versus PHA-680632 = 0.0002, $*P$ versus vehicle <0.0001). (b) Combination of PHA-680632 with dasatinib significantly increases the percentage of cell death after cytokinesis with failed reattachment ($*P < 0.0001$ versus all other treatment groups). (c) Representative western analysis comparing induction of apoptotic markers (cleaved PARP, cleaved caspase-3) at 48 h after growth of cells on tissue culture plastic versus in suspension, under the conditions of drug treatment indicated.

condensation, in live-cell imaging experiments focusing on GFP-H2B, to visualize chromatin. We followed the fate of individual cells for up to 48 h following release from thymidine block, and categorized cell death as (1) death without mitotic entry, (2) death in mitosis, (3) death of one or both daughter cells produced from an apparently normal mitosis and (4) death of a multinuclear daughter cell produced after an aberrant mitosis (Supplementary Figure S2). Compared with vehicle or the individual drug treatments, the majority of cell deaths following treatment with the combination of PHA-680632 and dasatinib followed an aberrant mitosis ($72.3\% \pm 6.3$ for the combination versus $46.2\% \pm 19.6$ for PHA-680632 ($P < 0.0001$), $9.5\% \pm 8.2$ for vehicle, and $5.6 \pm 9.6\%$ for dasatinib) (Figure 4a). However, death was not an immediate consequence of mitosis, but occurred typically 10–13 h later, with no difference in timing between treatment groups (Supplementary Figure S3A).

The SRC family kinases targeted by dasatinib are important for both cell attachment and control of mitotic cell rounding (Mustelin and Hunter, 2002; Yeatman, 2004). We evaluated the bright field images from the live-cell imaging experiment and stratified the cells that underwent cell death as follows: (1) attached cells that did not undergo mitotic division, (2) cells that lost attachment and did not undergo division, (3) cells that entered mitosis with normal postmitotic reattachment and (4) cells that entered mitosis but displayed post-mitotic reattachment failure (Supplementary Figure S2). Strikingly, a large percentage of cells treated

with PHA-680632 plus dasatinib that died failed to re-spread after mitosis, a death phenotype not significantly represented with either vehicle or individual drug-treated cells (Figure 4b). The latency between initial cell rounding for mitosis and cell death was similar among all the treatment groups (Supplementary Figure S3B); rather, the drug combination selectively increased the percentage of the cell population undergoing this fate.

These data implied that the interaction between PHA-680632 and dasatinib depended on disruption of cell attachment. To test this idea, we compared the efficacy of this drug combination in adherent cells, versus cells growing in detached conditions. We found that cell death was not significantly elevated in suspension cells treated with the drug combination versus either alone (Figure 4c), supporting the interpretation that disruption of adhesive signals was an important component of the drug interaction.

Functional and direct interactions between SRC and AURKA

We next assessed whether AURKA and SRC directly or functionally interact, so that inhibition of one might depress activation of the other, contributing to the observed synergy in growth inhibition. We determined that treatment of cells with dasatinib did not inhibit AURKA activity in OVCAR10 cells (Figure 5a). Reciprocally, PHA-680632 has no effect on SRC activity at the highest concentrations used in this study (Figures 5b and Supplementary Figure S4). However, PHA-680632 significantly potentiated dasatinib in

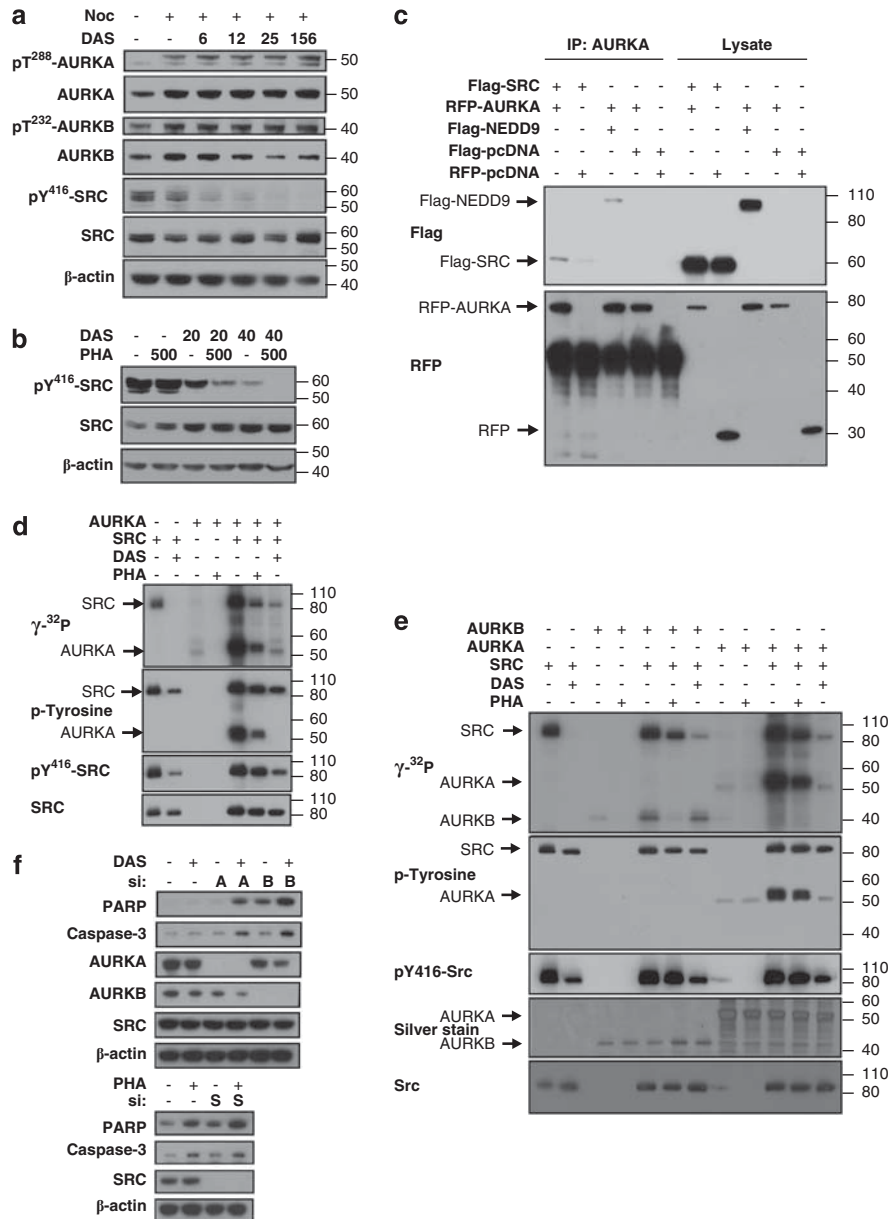


Figure 5 Physical and functional interaction of SRC and AURKA kinase. **(a)** Dasatinib inhibits SRC in a dose-dependent manner but does not have any effects on nocodazole-induced activation of AURKA or AURKB. AURKA was pre-activated as described in Kaestner *et al.* (2009), then cells were either unsynchronized or synchronized with 300 nM nocodazole (Sigma-Aldrich) for 12 h and then treated with increasing doses of dasatinib for 3 h. **(b)** Western blot of whole cell lysates from OVCAR10 cells treated for 4 h with vehicle (DMSO), 500 nM PHA-680632, 20 or 40 nM dasatinib or the combination of PHA-680632 with dasatinib. **(c)** Overexpressed FLAG-SRC interacts with overexpressed AURKA. Cell lysates from HEK-293T cells transfected with constructs overexpressing the indicated proteins were immunoprecipitated with AURKA-conjugated agarose beads, and probed by western blot. **(d)** *In vitro* kinase assay with recombinant SRC and AURKA, with phosphorylation visualized by autoradiography with γ -³²P-ATP, then re probed with phosphosite-directed antibodies as indicated. For this and panel (f), drugs were added 20 min before initiation of assay by addition of ATP. 500 nM dasatinib and 1000 nM PHA-680632 were used in these experiments. **(e)** *In vitro* kinase assay with recombinant purified SRC, AURKA and AURKB as indicated. 500 nM dasatinib and 500 nM PHA-680632 were used in these experiments. Visualization of phosphorylation as in (d, f) Cells were treated with siRNA to deplete SRC (S), AURKA (A), or AURKB (B), or with scrambled control siRNA (–), in combination with vehicle, dasatinib or PHA-680632, as indicated. Representative western blot indicates degree of depletion, and appearance of cleaved PARP or caspase-3 as indications of apoptosis.

blocking SRC activation, as gauged by either western blot (Figure 5b) or immunofluorescence assays (Supplementary Figure S4). In further analysis, we found that SRC and AURKA co-immunoprecipitated following co-expression of tagged constructs (Figure 5c). This interaction was similar to the levels seen with

positive control NEDD9, supporting the idea of a potential interaction; however, to date we have not observed co-immunoprecipitation of endogenous SRC and AURKA.

To further probe AURKA and SRC interactions, we next performed an *in vitro* kinase assay with the two

kinases (Figure 5d). The auto-phosphorylation seen with recombinant SRC alone and recombinant AURKA alone is blocked by dasatinib and PHA-680632, respectively. When SRC and AURKA are combined in the same kinase reaction, we detect a very large increase in phosphorylation of both SRC and AURKA, an effect that is only partially blocked by either PHA-680632 or dasatinib treatment. Interestingly, combination of SRC and AURKA induced significant phospho-tyrosine staining on AURKA (Figure 5d), indicative of SRC substrate specificity. In contrast, combination of SRC and AURKB did not increase in auto-phosphorylation by SRC, and SRC did not tyrosine-phosphorylate AURKB, while only weakly inducing AURKB auto-phosphorylation (Figure 5e).

To further probe the specificity of SRC and Aurora kinase interactions, we examined induction of apoptosis in cells treated with dasatinib plus small interfering RNAs (siRNAs) targeting AURKA versus AURKB, or with PHA-680632 plus siRNA targeting SRC (Figure 5f). Depletion of AURKA and AURKB independently increased PARP and caspase-3 cleavage in conjunction with dasatinib. Although a greater absolute magnitude of PARP induction was observed with AURKB, this was on a background, in which siRNA to AURKB itself significantly induced PARP; in contrast, siRNA to AURKA only induced apoptotic signaling when combined with dasatinib. Interestingly, in the context of dasatinib treatment, siRNA depletion of AURKB led to cross-depletion of AURKA, and inhibition of AURKA cross-depleted AURKB, again suggesting dialog between the dasatinib targets and these proteins. SiRNA to SRC in combination with PHA-680632 also led to greater co-induction of PARP, although not to the same extent as with the siAurora/dasatinib combinations. The lesser effect may be due to the presence of multiple other SRC family members, such as LYN, YES and FYN, in ovarian cancer cells, which would be inhibited by dasatinib but not siRNA; or by inhibition of an alternative dasatinib target.

Discussion

We have here described a novel *in vitro* synergy between dasatinib and inhibitors of Aurora kinases in ovarian and colorectal cancer cell lines, but not in normal ovarian epithelial cells, and we have shown that multiple drugs that inhibit SRC family kinases and Aurora kinases have similar phenotypes. Treatment of cells with combined AURKA inhibitors and dasatinib resulted in a specific elimination of aneuploid cells after they have undergone defective mitosis and failed to reattach to substrate. SRC and AURKA directly interacted *in vitro*, and administration of PHA-680632 in conjunction with treatment with dasatinib potentiated reduction of SRC kinase activity.

Both dasatinib and Aurora inhibitors are showing promise in the clinic for treatment of some malignancies. For example, in chronic myeloid leukemia, dasatinib treatment has resulted in high rates of complete

cytogenic response, where tumor cells are no longer detected in the blood of patients, both after failure of imatinib treatment (Hochhaus *et al.*, 2008) and as a first-line treatment (Kantarjian *et al.*, 2010), based on the activity of this compound against BCR-ABL. Phase I data showed that treatment with the pan-Aurora inhibitor PHA-739358 resulted in clinically relevant disease stabilization in some patients, and a phase II study recently demonstrated that complete hematological response can be reached in two of 12 patients with chronic myeloid leukemia (Boss *et al.*, 2009). Our data support the combined use of such compounds may be worth exploring in the clinic. Interestingly, Fei *et al.* (2010) reported that combined treatment of Philadelphia chromosome-positive human acute lymphoblastic leukemia cells with a combination of the pan-Aurora inhibitor VX-680 and dasatinib resulted in a significant increase in cytotoxicity compared with the individual drugs alone. As VX-680 also has been shown to inhibit the BCR-ABL oncoprotein based on off-target activity (Carter *et al.*, 2005), the authors attribute synergy to potent inhibition of this oncogenic fusion protein. Our data suggest that inhibition of Aurora kinases and SRC may also contribute, particularly as Fei *et al.* (2010) noted a more significant reduction in phospho-SRC when ALL cells were treated with a combination of dasatinib and VX-680 as compared with the individual agents, although they did not pursue this observation. It will be informative to assess whether VX-680/dasatinib synergy is observed in solid tumors, in which BCR-ABL is not a driving lesion. Interestingly, in previous work, we found dual inhibition of AURKA and the receptor tyrosine kinase EGFR significantly and selectively reduced the activity of SRC and other SRC-family kinases (FGR, HCK, LYN and LCK) (Astsaturov *et al.*, 2010), further implying close signaling interactions between AURKA, SRC and another important therapeutic target.

The idea of dually targeting SRC and Aurora inhibitors has potentially greater impact than suggesting new applications for dasatinib. Multiple SRC inhibitors are currently undergoing clinical trials. These include not only the ATP-binding site-competitive inhibitors such as dasatinib and AZD0530, but also substrate-binding site inhibitors such as KXOI (Kopetz *et al.*, 2007; Guarino, 2010). There have been some clinical successes with these agents. However, despite their promise, SRC inhibitors used as single agents in preclinical models and phase I trials have been shown to only affect proliferation in a very limited number of cases (Jones *et al.*, 2002; Johnson *et al.*, 2005), and do not effectively induce tumor regression based on radiographic analysis (Kopetz *et al.*, 2007). It would be of interest to also evaluate these for interaction with Aurora inhibitors.

Mechanistically, the death phenotype of dually treated cells indicates a failure to re-adhere after prior defects in completion of mitosis is an important component of the resulting apoptosis. There are many links between cellular attachment and cell division. Defective cellular attachment results in multinucleation,

and inhibition of cytokinesis in part because of failure of cells to generate adequate traction forces to drive separation (Ben-Zéev and Raz, 1981; Huang *et al.*, 2005; Orly and Sato, 1979). AURKA and SRC have each separately been shown to influence the completion of cytokinesis. SRC localized to plasma membrane subdomains at the cleavage furrow becomes hyper-phosphorylated at cytokinesis, with SRC activation supporting cleavage furrow progression (Ng *et al.*, 2005) and abscission (Kasahara *et al.*, 2007). Likewise, microinjection of antibodies to inhibit AURKA at metaphase was shown to prevent cytokinesis completion (Marumoto *et al.*, 2003). NEDD9, a physical interactor of both SRC and AURKA, relocalizes from focal adhesion complexes to the spindle asters during mitosis, and misexpression of NEDD9 leads to cytokinesis failure (Pugacheva and Golemis, 2005; Dadke *et al.*, 2006). Loss of adhesion is ultimately associated with anoikis in epithelial cells (Frisch and Screaton, 2001), due to loss of survival signals mediated through integrins. Our data are compatible with the idea that given the close interaction of AURKA, SRC and NEDD9, inhibition of two of these proteins simultaneously may exacerbate defects in both the cell division and cell survival processes they mediate.

Materials and methods

Cell lines, compounds and plasmids

The OVCAR10, OVCAR5 and OVCAR3 ovarian carcinoma cell lines and the HCT116 (*K-RAS* mutant, *TP53* wildtype) colorectal carcinoma cell line were obtained from the ATCC (Manassas, VA, USA). The DLD-1 (*K-RAS* mutant, *TP53* mutant) and DKS-8 (isogenic to DLD-1, but with the activated *K-RAS* allele disrupted (hence, *K-RAS* wild-type), *TP53* mutant) colorectal cancer cell lines were a kind gift of Dr Robert J Coffey (Vanderbilt University, TN, USA). Primary HOSE cells were isolated, characterized and cultured as previously described (Dyck *et al.*, 1996; Bellacosa *et al.*, 2010). All ovarian cancer cell lines were maintained in RPMI supplemented with 10% (v/v) fetal bovine serum and insulin, L-glutamine, penicillin and streptomycin. All colorectal cancer cell lines were maintained in DMEM supplemented with 10% (v/v) fetal bovine serum, L-glutamine, penicillin and streptomycin. Suspension cell culture was performed in six-well Ultra-low Attachment Surface plate (Corning Life Sciences, Pittston, PA, USA).

PP2 and C1368 were obtained from Sigma-Aldrich (St Louis, MO, USA); dasatinib was obtained from Bristol Myers Squibb (New York, NY, USA); AZD1152-HQPA was obtained from Selleck Chemicals (Houston, TX, USA); PHA-680632 was obtained from Nerviano Medical Sciences (Nerviano, Italy); MLN8237 was obtained from Millenium Pharmaceuticals (Greenwood Village, CO, USA). The Flag-Src plasmids were a kind gift of Dr Philip Stork (Oregon Health and Science University, OR, USA). A PCR product of mouse Red Fluorescent Protein (mRFP) was ligated into pcDNA3.1(+) (Invitrogen, Carlsbad, CA, USA) to create pcDNA3.1-mRFP. Aurora-A was expressed from pcDNA3.1-mRFP vectors; pcDNA3.1-mRFP was used as a negative control. Flag-fused HEF1/NEDD9 was expressed from the vector pCatch-FLAG (O'Neill and Golemis, 2001). On-TARGETplus SMARTpool siRNA oligos (Dharmacon, Lafayette,

CO, USA) were made against the following sequences: AURKA, J-003545 (5'-UCGAAGAGAGUUAUUCUAUA-3', 5'-CGGUAGGCCUGAUUGGGUU-3', 5'-UUCUUAGACUGUAUGGUUA-3', and 5'-AAUAGGAACACGUGCU CUA-3'); AURKB, J-003326 (5'-CCAAACUGCUCAGGCA UAA-3', 5'-ACGCGGCACUUCACAAUUG-3', 5'-GCGCA GAGAGAUCCGAAAUC-3', and 5'-CAGAAGAGCUGCA CAUUUG-3'); SRC, J-003175 (5'-GCAGUUGUAUGCUG UGGUU-3', 5'-GCAGAGAACCCGAGAGGGA-3', 5'-CCA AGGGCCUCAACGUGAA-3', and 5'-GGGAGAACCUCU AGGCACA-3').

Drug synergy testing

For each drug tested, initial IC₅₀ curves were established in each cell line to calibrate dose range for subsequent *in vitro* synergy experiments. For subsequent analysis, we used the ratio that shows the most significant drop in viability in the combined drug treatment compared with the individual drug treatment. Cells were plated at 2000 (ovarian cancer cell lines) to 3000 (colorectal cancer cell lines) cells/well into 96-well plates. After 24 h, vehicle (DMSO), individual drugs or drug combinations were added, followed by 72 h incubation. Cellular viability measurements were performed using the CellTiter Blue assay (Promega, Fitchburg, WI, USA). The coefficient of interaction (CI) between pharmacological inhibitors was established by the Chou–Talalay method (Chou and Talalay, 1984) using CalcuSyn software (Biosoft, Cambridge, UK).

Fluorescence-activated cell sorting analysis

Cells growing in 60 mm plates were synchronized overnight with 2 mM thymidine. At 3 h following release from the thymidine block, cells were treated with vehicle, PHA-680632, dasatinib or the combination of the two drugs. Attached and floating cells were harvested, fixed in 70% ethanol and stained with propidium iodide following standard protocols provided with the Guava Cell Cycle Reagent (Millipore, Billerica, MA, USA). Cell-cycle profiles were acquired using Guava flow cytometry at time periods noted after drug treatment.

Time-lapse video microscopy

Cells stably expressing green fluorescent protein-linked histone H2B (GFP-H2B) were seeded into six-well plates and 2 mM thymidine was added for 18 h, synchronizing the cells in G1/S phase. At 3 h following thymidine washout, cells were treated with vehicle (DMSO), or 500 nM PHA-680632, or 156 nM dasatinib, or 500 nM PHA-680632 plus 156 nM dasatinib. Cells were then placed into a heated chamber, and bright field and fluorescent images were taken every 5 min for up to 48 h using a Nikon TE2000 microscope (Nikon, Tokyo, Japan) controlled by Metamorph software (Molecular Devices, Sunnyvale, CA, USA). Stacks of individual movies were built and analyzed manually for the indicated measurements. A minimum of 90 cells was counted for each movie and experiments were conducted at least three times. For montages, selected frames representing different cell morphologies were chosen.

Western blotting, immunoprecipitation and immunofluorescence

Cell extracts were prepared using CellLytic-M Cell Lysis Reagent (Sigma-Aldrich) supplemented with the Halt phosphatase inhibitor cocktail (Thermo Scientific, Rockford, IL, USA) and the Complete Mini protease inhibitor cocktail (Roche Diagnostics GmbH, Mannheim, Germany). Extracts were centrifuged at 15 000 × *g* for 15 min at 4 °C. Immunopre-

precipitation assays were performed as described in (Obara *et al.*, 2004). Agarose-immobilized Aurora-A antibody (Bethyl Laboratories, Montgomery, TX, USA) was used for immunoprecipitation. Other antibodies used were directed against phospho-tyrosine, Aurora-B/AIM-1 and Aurora-A/IAK1 (BD Transduction Laboratories, San Jose, California, USA), GST (Santa Cruz Biotechnology, Santa Cruz, CA, USA), the Flag M2 epitope tag (Sigma-Aldrich), Red fluorescent protein (RFP) (US Biological, Marblehead, MA, USA), and the PARP 214/215 cleavage site (Millipore). Secondary anti-mouse or anti-rabbit horseradish peroxidase coupled antibodies were purchased from GE Healthcare (Little Chalfont, Buckinghamshire, UK). All remaining antibodies used in western blot experiments (to phospho-Y⁴¹⁶ Src, Src, phospho-T²⁸⁸ Aurora-A, pan-phospho Aurora (recognizing phosphorylation on AURKA-T²⁸⁸/AURKB-T²³²/AURKC-T¹⁹⁸), and β -actin), cleaved caspase-3 (D¹⁷⁵) were purchased from Cell Signaling (Danvers, MA, USA). Phospho-Y⁴¹⁶ Src antibody (Invitrogen, Carlsbad, CA, USA) and Alexa-Fluor anti-rabbit and anti-mouse secondary antibodies (Invitrogen) were used for immunofluorescence.

In vitro kinase assays

In vitro kinase assays were performed using recombinant active Aurora A (Millipore), recombinant Hexa-histidine baculovirus-produced Aurora A, recombinant active Aurora B (Millipore), or recombinant active Src kinase (Cell Signaling). Bacterially expressed GST-fused NEDD9₁₋₃₆₃ (produced in BL21 bacteria, as described in Pugacheva and Golemis (2005) and GST protein were added to reactions as indicated. For drug inhibition experiments, recombinant proteins were pretreated with drugs on ice for 20 min before the start of the kinase reaction. *In vitro* kinase reaction was performed with γ -³²P-ATP (Perkin-Elmer, Waltham, MA, USA) as in Pugacheva and Golemis (2005). All assays were carried out a minimum of three times and a representative blot is shown in experiments.

Clonogenic and matrigel assays

For clonogenic assays, cells were plated at concentration of 1000 cells per 35 mm dish, and after 24 h treated with vehicle (DMSO) PHA-680632, dasatinib or drug combination for 24 h. Subsequently, cells were cultured in fresh media without drugs for 10–12 days. Colonies were fixed with 4% paraformaldehyde/phosphate-buffered saline, and stained with 0.4% crystal violet/20% methanol. Colonies larger than 10 pixels in diameter (typically ~8 cells) were counted with Metamorph software. For 3D matrigel assays, 5×10^3 OVCAR10 cells were

added to 40 μ l of growth factor-reduced matrigel in eight-well Lab-Tek chamber slides (Nunc, Rochester, NY, USA). After 4 days, drugs were added in fresh medium, and cell maintained for 8 days before fixation in 4% paraformaldehyde, followed by immunofluorescence or staining with crystal violet.

Statistical methods

A Chi-square test was used to compare cell counts for different phenotypic categories among the four drug treatment types in time-lapse microscopy experiments. The Chi-square test was also used to test the type of cell division that was induced by drug treatments. The time of entry into mitosis was compared across the treatment types via the log-rank test. The duration of mitosis was compared across the treatment types via the non-parametric Wilcoxon test. Overall equality of several proportions for fraction of cell deaths and types of cell deaths over the drug treatment groups were submitted to permutation tests. Fluorescence-activated cell sorting data were analyzed using a two-tailed Student's *t*-test. Clonogenic survival and matrigel assay data were analyzed using a one-tailed Student's *t*-test.

Conflict of interest

The authors declare no conflict of interest.

Acknowledgements

We thank Lisa Vanderveer for assistance with maintaining EOC cell lines; Carolyn Slater for isolating and producing the primary HOSE cultures; Christine Klimowicz for assistance with the drug synergy assays; and Ilya Serebriiskii for assistance with editing the figures. This work was supported by R01-CA63366 and R01-CA113342; DOD W81XWH-07-1-0676 from the Army Materiel Command; and Tobacco Settlement funding from the State of Pennsylvania (to EAG); R01-CA140323 and the Ovarian Cancer Research Fund (to AKG); Ovarian SPORE P50 CA083638 (Project 4, to EAG, AKG, and DCC); R01-GM86877, an appropriation from the Commonwealth of Pennsylvania, and the Greenberg Fund (to TJY); R01-CA136596 and R01-CA151374 (to DCC); R01-CA50633 (to LMW); and by NCI CA06927 and support from the Pew Charitable Fund (to Fox Chase Cancer Center). Additional funds were provided by Fox Chase Cancer Center via institutional support of the Head and Neck Cancer Keystone Program.

References

- Anand S, Penrhyn-Lowe S, Venkitaraman AR. (2003). AURORA-A amplification overrides the mitotic spindle assembly checkpoint, inducing resistance to Taxol. *Cancer Cell* **3**: 51–62.
- Astsaturov I, Ratushny V, Sukhanova A, Einarson MB, Bagnyukova T, Zhou Y *et al.* (2010). Synthetic lethal screen of an EGFR-centered network to improve targeted therapies. *Sci Signal* **3**: ra67.
- Bagnyukova TV, Serebriiskii IG, Zhou Y, Hopper-Borge EA, Golemis EA, Astsaturov I. (2010). Chemotherapy and signaling: How can targeted therapies supercharge cytotoxic agents? *Cancer Biol Ther* **10**: 839–853.
- Bellacosa A, Godwin AK, Peri S, Devarajan K, Caretti E, Vanderveer L *et al.* (2010). Altered gene expression in morphologically normal epithelial cells from heterozygous carriers of BRCA1 or BRCA2 mutations. *Cancer Prev Res (Phila)* **3**: 48–61.
- Ben-Zéev A, Raz A. (1981). Multinucleation and inhibition of cytokinesis in suspended cells: reversal upon reattachment to a substrate. *Cell* **26**: 107–115.
- Bischoff JR, Anderson L, Zhu Y, Mossie K, Ng L, Souza B *et al.* (1998). A homologue of Drosophila aurora kinase is oncogenic and amplified in human colorectal cancers. *Embo J* **17**: 3052–3065.
- Boss DS, Beijnen JH, Schellens JH. (2009). Clinical experience with aurora kinase inhibitors: a review. *Oncologist* **14**: 780–793.
- Brandsma D, van den Bent MJ. (2007). Molecular targeted therapies and chemotherapy in malignant gliomas. *Curr Opin Oncol* **19**: 598–605.
- Cao Y, Liu Q. (2007). Therapeutic targets of multiple angiogenic factors for the treatment of cancer and metastasis. *Adv Cancer Res* **97**: 203–224.

- Carter TA, Wodicka LM, Shah NP, Velasco AM, Fabian MA, Treiber DK *et al.* (2005). Inhibition of drug-resistant mutants of ABL, KIT, and EGF receptor kinases. *Proc Natl Acad Sci U S A* **102**: 11011–11016.
- Chou TC, Talalay P. (1984). Quantitative analysis of dose-effect relationships: the combined effects of multiple drugs or enzyme inhibitors. *Adv Enzyme Regul* **22**: 27–55.
- Dadke D, Jarnik M, Pugacheva EN, Singh MK, Golemis EA. (2006). Deregulation of HEF1 impairs M-phase progression by disrupting the RhoA activation cycle. *Mol Biol Cell* **17**: 1204–1217.
- Ditchfield C, Johnson VL, Tighe A, Ellston R, Haworth C, Johnson T *et al.* (2003). Aurora B couples chromosome alignment with anaphase by targeting BubR1, Mad2, and Cenp-E to kinetochores. *J Cell Biol* **161**: 267–280.
- Dutertre S, Descamps S, Prigent C. (2002). On the role of aurora-A in centrosome function. *Oncogene* **21**: 6175–6183.
- Dyck HG, Hamilton TC, Godwin AK, Lynch HT, Maines-Bandiera S, Auersperg N. (1996). Autonomy of the epithelial phenotype in human ovarian surface epithelium: changes with neoplastic progression and with a family history of ovarian cancer. *Int J Cancer* **69**: 429–436.
- Fei F, Stoddart S, Groffen J, Heisterkamp N. (2010). Activity of the Aurora kinase inhibitor VX-680 against Bcr/Abl-positive acute lymphoblastic leukemias. *Mol Cancer Ther* **9**: 1318–1327.
- Fernandez-Miranda G, Trakala M, Martin J, Escobar B, Gonzalez A, Ghyselinck NB *et al.* (2011). Genetic disruption of aurora B uncovers an essential role for aurora C during early mammalian development. *Development* **138**: 2661–2672.
- Friedman A, Perrimon N. (2007). Genetic screening for signal transduction in the era of network biology. *Cell* **128**: 225–231.
- Frisch SM, Screaton RA. (2001). Anoikis mechanisms. *Curr Opin Cell Biol* **13**: 555–562.
- Gautschi O, Heighway J, Mack PC, Purnell PR, Lara Jr PN, Gandara DR. (2008). Aurora kinases as anticancer drug targets. *Clin Cancer Res* **14**: 1639–1648.
- Giet R, Petretti C, Prigent C. (2005). Aurora kinases, aneuploidy and cancer, a coincidence or a real link? *Trends Cell Biol* **15**: 241–250.
- Glover DM, Leibowitz MH, McLean DA, Parry H. (1995). Mutations in aurora prevent centrosome separation leading to the formation of monopolar spindles. *Cell* **81**: 95–105.
- Guan Z, Wang XR, Zhu XF, Huang XF, Xu J, Wang LH *et al.* (2007). Aurora-A, a negative prognostic marker, increases migration and decreases radiosensitivity in cancer cells. *Cancer Res* **67**: 10436–10444.
- Guarino M. (2010). Src signaling in cancer invasion. *J Cell Physiol* **223**: 14–26.
- Hochhaus A, Baccarani M, Deininger M, Apperley JF, Lipton JH, Goldberg SL *et al.* (2008). Dasatinib induces durable cytogenetic responses in patients with chronic myelogenous leukemia in chronic phase with resistance or intolerance to imatinib. *Leukemia* **22**: 1200–1206.
- Huang X, Dai W, Darzynkiewicz Z. (2005). Enforced adhesion of hematopoietic cells to culture dish induces endomitosis and polyploidy. *Cell Cycle* **4**: 801–805.
- Johnson FM, Saigal B, Talpaz M, Donato NJ. (2005). Dasatinib (BMS-354825) tyrosine kinase inhibitor suppresses invasion and induces cell cycle arrest and apoptosis of head and neck squamous cell carcinoma and non-small cell lung cancer cells. *Clin Cancer Res* **11**: 6924–6932.
- Jones RJ, Avizienyte E, Wyke AW, Owens DW, Brunton VG, Frame MC. (2002). Elevated c-Src is linked to altered cell-matrix adhesion rather than proliferation in KM12C human colorectal cancer cells. *Br J Cancer* **87**: 1128–1135.
- Kaestner P, Stolz A, Bastians H. (2009). Determinants for the efficiency of anticancer drugs targeting either Aurora-A or Aurora-B kinases in human colon carcinoma cells. *Mol Cancer Ther* **8**: 2046–2056.
- Kantarjian H, Shah NP, Hochhaus A, Cortes J, Shah S, Ayala M *et al.* (2010). Dasatinib versus imatinib in newly diagnosed chronic-phase chronic myeloid leukemia. *N Engl J Med* **362**: 2260–2270.
- Kasahara K, Nakayama Y, Nakazato Y, Ikeda K, Kuga T, Yamaguchi N. (2007). Src signaling regulates completion of abscission in cytokinesis through ERK/MAPK activation at the midbody. *J Biol Chem* **282**: 5327–5339.
- Keen N, Taylor S. (2004). Aurora-kinase inhibitors as anticancer agents. *Nat Rev Cancer* **4**: 927–936.
- Kopetz S, Shah AN, Gallick GE. (2007). Src continues aging: current and future clinical directions. *Clin Cancer Res* **13**: 7232–7236.
- Lombardo LJ, Lee FY, Chen P, Norris D, Barrish JC, Behnia K *et al.* (2004). Discovery of N-(2-chloro-6-methyl-phenyl)-2-(6-(4-(2-hydroxyethyl)-piperazin-1-yl)-2-methylpyrimidin-4-ylamino)thiazole-5-carboxamide (BMS-354825), a dual Src/Abl kinase inhibitor with potent antitumor activity in preclinical assays. *J Med Chem* **47**: 6658–6661.
- Marumoto T, Honda S, Hara T, Nitta M, Hirota T, Kohmura E *et al.* (2003). Aurora-A kinase maintains the fidelity of early and late mitotic events in HeLa cells. *J Biol Chem* **278**: 51786–51795.
- Minegishi M, Tachibana K, Sato T, Iwata S, Nojima Y, Morimoto C. (1996). Structure and function of Cas-L, a 105-kD Crk-associated substrate-related protein that is involved in beta-1 integrin-mediated signaling in lymphocytes. *J Exp Med* **184**: 1365–1375.
- Mustelin T, Hunter T. (2002). Meeting at mitosis: cell cycle-specific regulation of c-Src by RPTPalph. *Sci STKE* **2002**: pe3.
- Ng MM, Chang F, Burgess DR. (2005). Movement of membrane domains and requirement of membrane signaling molecules for cytokinesis. *Dev Cell* **9**: 781–790.
- O'Neill GM, Golemis EA. (2001). Proteolysis of the docking protein HEF1 and implications for focal adhesion dynamics. *Mol Cell Biol* **21**: 5094–5108.
- Obara Y, Labudda K, Dillon TJ, Stork PJ. (2004). PKA phosphorylation of Src mediates Rap1 activation in NGF and cAMP signaling in PC12 cells. *J Cell Sci* **117**: 6085–6094.
- Orly J, Sato G. (1979). Fibronectin mediates cytokinesis and growth of rat follicular cells in serum-free medium. *Cell* **17**: 295–305.
- Pfeiffer P, Qvortrup C, Eriksen JG. (2007). Current role of antibody therapy in patients with metastatic colorectal cancer. *Oncogene* **26**: 3661–3678.
- Plotnikova OV, Golemis EA. (2011). Aurora-A kinase activity influences calcium signaling in kidney cells. *J Cell Biol* **193**: 1021–1032.
- Plotnikova OV, Pugacheva EN, Dunbrack RL, Golemis EA. (2010). Rapid calcium-dependent activation of Aurora-A kinase. *Nat Commun* **1**: 1–8.
- Pugacheva EN, Golemis EA. (2005). The focal adhesion scaffolding protein HEF1 regulates activation of the Aurora-A and Nek2 kinases at the centrosome. *Nat Cell Biol* **7**: 937–946.
- Pugacheva EN, Jablonski SA, Hartman TR, Henske EP, Golemis EA. (2007). HEF1-dependent Aurora A activation induces disassembly of the primary cilium. *Cell* **129**: 1351–1363.
- Shor AC, Keschman EA, Lee FY, Muro-Cacho C, Letson GD, Trent JC *et al.* (2007). Dasatinib inhibits migration and invasion in diverse human sarcoma cell lines and induces apoptosis in bone sarcoma cells dependent on SRC kinase for survival. *Cancer Res* **67**: 2800–2808.
- Soncini C, Carpinelli P, Gianellini L, Fancelli D, Vianello P, Rusconi L *et al.* (2006). PHA-680632, a novel Aurora kinase inhibitor with potent antitumor activity. *Clin Cancer Res* **12**: 4080–4089.
- Wong ST, Goodin S. (2009). Overcoming drug resistance in patients with metastatic breast cancer. *Pharmacotherapy* **29**: 954–965.
- Yeatman TJ. (2004). A renaissance for SRC. *Nat Rev Cancer* **4**: 470–480.

Supplementary Information accompanies the paper on the Oncogene website (<http://www.nature.com/onc>)